


Article

An Accelerated Degradation Durability Evaluation Model for the Turbine Impeller of a Turbine Based on a Genetic Algorithms Back-Propagation Neural Network

Xiaojian Yi ^{1,2,*} , Zhezhe Wang ¹, Shulin Liu ³, Xinrong Hou ⁴ and Qing Tang ³¹ School of Mechatronical Engineering, Beijing Institute of Technology, Beijing 100081, China² Yangtze Delta Region Academy of Beijing Institute of Technology, Jiaxing 314003, China³ Quality and Reliability Center, China Institute of Marine Technology and Economy, Beijing 100081, China⁴ China North Engine Research Institute, Tianjin 300400, China

* Correspondence: yixiaojianbit@sina.cn

Abstract: Durability evaluation plays an important role in product operation and maintenance during the design stage. In order to ensure a long life, high reliability, and short development cycle, an accelerated degradation durability evaluation model for the turbine impeller of a turbine based on a genetic algorithms back-propagation neural network is established. Based on the proposed model, we discuss two types of practical problems. One is the matching problem of the component strengthening test and whole machine system test. The other is the design problem of two kinds of bench tests. All in all, this work not only proposes a durability evaluation model to effectively solve the current turbine durability evaluation problems, but it also provides a feasible research idea for similar problems.

Keywords: accelerated degradation model; durability evaluation; back-propagation neural network



Citation: Yi, X.; Wang, Z.; Liu, S.; Hou, X.; Tang, Q. An Accelerated Degradation Durability Evaluation Model for the Turbine Impeller of a Turbine Based on a Genetic Algorithms Back-Propagation Neural Network. *Appl. Sci.* **2022**, *12*, 9302. <https://doi.org/10.3390/app12189302>

Academic Editor: Andrea Prati

Received: 23 August 2022

Accepted: 13 September 2022

Published: 16 September 2022

Publisher's Note: MDPI stays neutral with regard to jurisdictional claims in published maps and institutional affiliations.



Copyright: © 2022 by the authors. Licensee MDPI, Basel, Switzerland. This article is an open access article distributed under the terms and conditions of the Creative Commons Attribution (CC BY) license (<https://creativecommons.org/licenses/by/4.0/>).

1. Introduction

A turbocharger is a key component of a special vehicle engine. If any part of a turbocharger fails, there will be serious consequences. Therefore, in the development stage, the durability assessment and evaluation of a turbocharger are crucial [1,2]. Many studies have shown that a turbine impeller is an important key component and is an important link in determining a turbocharger's durability. At present, for the development of long-life and high-reliability products, it is difficult to obtain a durability test verification conclusion within the development cycle according to the traditional test method, which cannot meet the product development needs. Therefore, it is necessary to speed up the test process and shorten the test time. Until now, the current durability assessment has mainly been based on failure data and performance degradation data. Assessment of the former is too dependent on failure data. In addition, the data is difficult to obtain due to the limited sample size and limited development cycle. To remedy the problem that traditional methods have—difficulty analyzing highly reliable products that lack failure data—scholars began to study the analysis methods based on performance degradation data, and it gradually become a hot topic [3].

As a study that analyzes methods based on performance degradation data, this research mainly focuses on the regression model, degradation distribution, and stochastic processes. The regression model uses regression fitting to obtain the product degradation trajectory through statistical analysis of the degradation data, and it mainly includes the failure physical model [4–6] and data fitting model [7–9]. The degradation distribution is used to determine the suitable degradation amount distribution function, such as the commonly used lognormal distribution [10] and Weibull distributions [11–13]. Based on these distribution functions, the parameter can be estimated and the degradation trajectory

model can be determined. Furthermore, the stochastic process can describe the randomness of the degradation path caused by internal and external influences in the product degradation process, and the popular stochastic process models include the Wiener process [14–16] and Gamma process [17–20]. In their studies on the durability evaluations of turbine impellers, Li et al. [21] and Zhu et al. [22] described the performance degradation processes of turbine impellers by developing a physical model of their failures. Zhou et al. [23] and Yue et al. [24] characterized the turbine impeller performance degradation law by the cumulative damage model and developed a corresponding fatigue life prediction model. Zhang et al. [25] established a nonlinear degradation model of a turbine impeller through neural network regression. Zhao et al. [26] used the Wiener process to establish a competitive failure model of an impeller to provide a basis for maintenance and reliability studies of the related components. Nonetheless, this research evaluates the product design life of a turbine impeller. In engineering practice, two types of tests are carried out in the process of turbine development (due to the limitation of the development cycle and cost): one is for the component-level structure strengthening assessment test of the turbine, and the other is a performance assessment test for the components installed on the whole machine. A turbine-related durability assessment has the following practical problems:

Problem I is the matching problem of the component strengthening test and whole machine system test. According to the component-level structural strengthening test, for example, in China, the test for a supercharger for special vehicles, the Turbocharger 120-h Structural Assessment Test Syllabus, is a type of strengthening test. It is also the national military standard for a 350-h complete test of the whole performance assessment test. The reinforcement test is a qualitative assessment method used to find the weak link in a product by rapidly increasing the test stress, while finding a way to using the shortest time to efficiently stimulate failure. However, it is difficult to meet the quantitative verification of the durability level of the supercharger, and whether or not the supercharger 120-h structural assessment test meets the requirements of the 350-h complete test does not have a clear mathematical explanation.

Problem II is the design problem of the two kinds of bench tests. The whole engine bench test time is no longer carried out according to the traditional method, such as when testing a special engine with a whole bench test from 350 h to 500 h of change, and how to provide an improved scientific basis for a supercharger structure assessment test has become an urgent problem.

Therefore, for a special vehicle turbine, this paper aims to establish an accelerated degradation durability evaluation model to solve the above two types of problems. The contributions of this paper are as follows:

(1) Based on GA-BP neural network for degradation data (bench test phase), we first propose a durability assessment model which can effectively avoid the problem of the complicated process of resolving multi-dimensional equation systems. Furthermore, the non-linear relationship between multiple stresses and the amount of performance degradation can be well mapped.

(2) We propose an effective way to solve the above two types of problems, and it can be used to guide solutions to similar problems.

The remaining structure of the article is as follows: Combined with the turbine-related bench test, the degradation parameters and sensitive parameters required by the accelerated degradation model are selected in Section 2. Section 3 proposes a turbine accelerated degradation durability assessment model based on a GA-BP neural network for assessing the turbine endurance limit. Section 4 discusses both the validity of the model and the application of the model, explaining the problems faced by the durability assessment as described above. Section 5 is the conclusion.

2. Characterization Parameters of the Turbine Impeller Degradation Failure Mechanism for a Bench Test

2.1. Failure Mechanism and Sensitive Stress Analysis

The deformation, fracture, and wear of turbine impellers are typical faults of turbochargers, and they will directly affect a turbocharger's performance and service life. The failure of a turbocharger turbine impeller has the characteristics of diversification and multiple parts due to the combined effect of centrifugal load, thermal load, and pneumatic load. Centrifugal loads make a turbine's blades subject to tensile stresses. A thermal load makes a turbine's blades produce thermal stress. A pneumatic load makes a turbine's blades' surface subject to gas pressure. Wang et al. [27] analyzed the effects of the three kinds of loads on the stress state of turbine blades, and they also analyzed the stress distribution state of turbine blades under the combined action of loads. From this study, it can be found that the effect of aerodynamic loads on the stress distribution of turbine blades is small and can generally be ignored. The major influences on the stress distribution of turbine blades are centrifugal load and thermal load. This paper takes a type of supercharger turbine as an example and uses ANSYS Multiphysics simulation software to establish a three-dimensional analysis model. Then, it analyzes the simulation model through the thermal-structural coupling module, which divides the mesh for the model, uses PLANE 55 cells to realize the coupling, and loads the temperature and speed conditions. The stress-strain distribution of the turbine under thermal and centrifugal loads, as shown in Figure 1, is obtained. From Figure 1, we can see that the maximum stress should be in the root of the turbine blade. Through the above analysis, and combined with the actual working environment of the turbine blade, it can be concluded that the root of the turbine blade is prone to fracturing under the fatigue and persistent loads.

C: Static Structural

Type: Equivalent Elastic Stress

Unit: MPa

Time: 1

Max: 824.63

Min: 2.0784

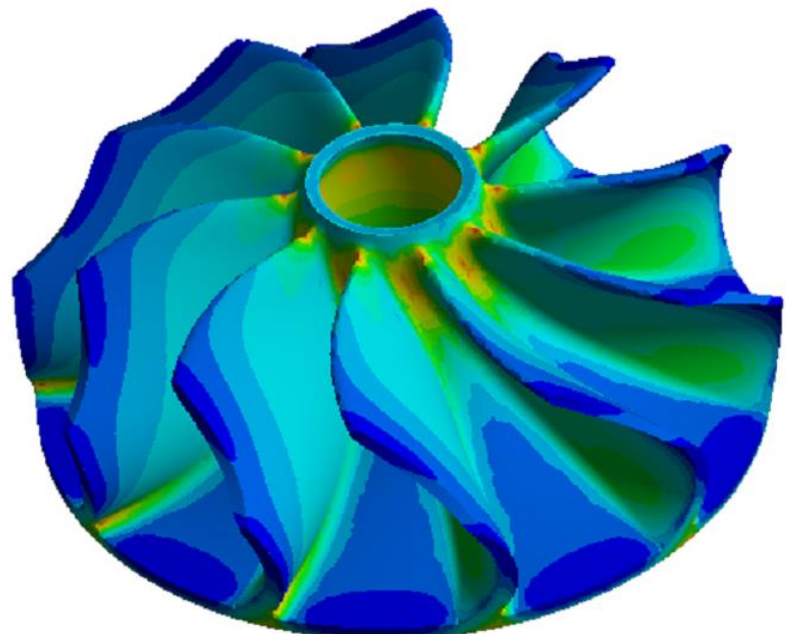
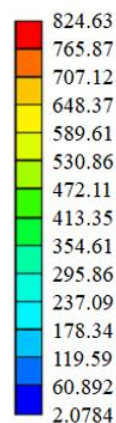


Figure 1. Cont.

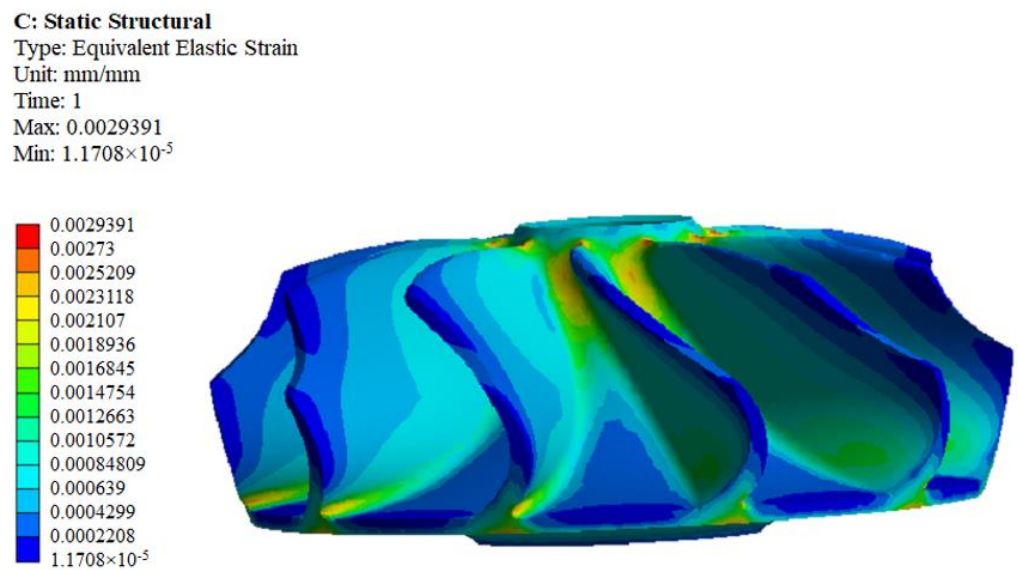


Figure 1. Stress distribution of turbine blades under centrifugal loads and thermal loads.

2.2. Determining the Sensitive Stress

A turbine is mainly subjected to the 120-h structural strengthening assessment test and the 350-h complete engine performance assessment test. The former test’s profile is shown in Figure 2, and the latter is based on the diesel engine durability test profile specified in the Chinese national military standard. As shown in Table 1, there are 35 cycles every 10 h.

Table 1. The 350-h engine complete test profile.

Sub Circulation	Calibration RPM	Torque (N·m)	Time (min)	Requirement
1		Start		Gradually increase the RPM, load, cooling medium, and oil temperature to meet the specified requirements.
2	Increase from the lowest no-load RPM to the highest no-load RPM three times			
3	100%	By external properties	60	Every 1 h to reduce the amount of oil supply and to reduce the speed of cooling, and the load switch remains unchanged and the speed of rotation slows down to the lowest stable operating speed, which is timed for 2–3 min (not counted in the assessment time).
4	85%~90%	By external properties	420	
5	80%	By external properties	100	
6	Maximum torque RPM	Maximum torque	20	
7	Check minimum no-load RPM			
8		Cooled parking		Gradually cool the diesel engine to the stopping specifications
9	The parking time is no more than 60 min.			

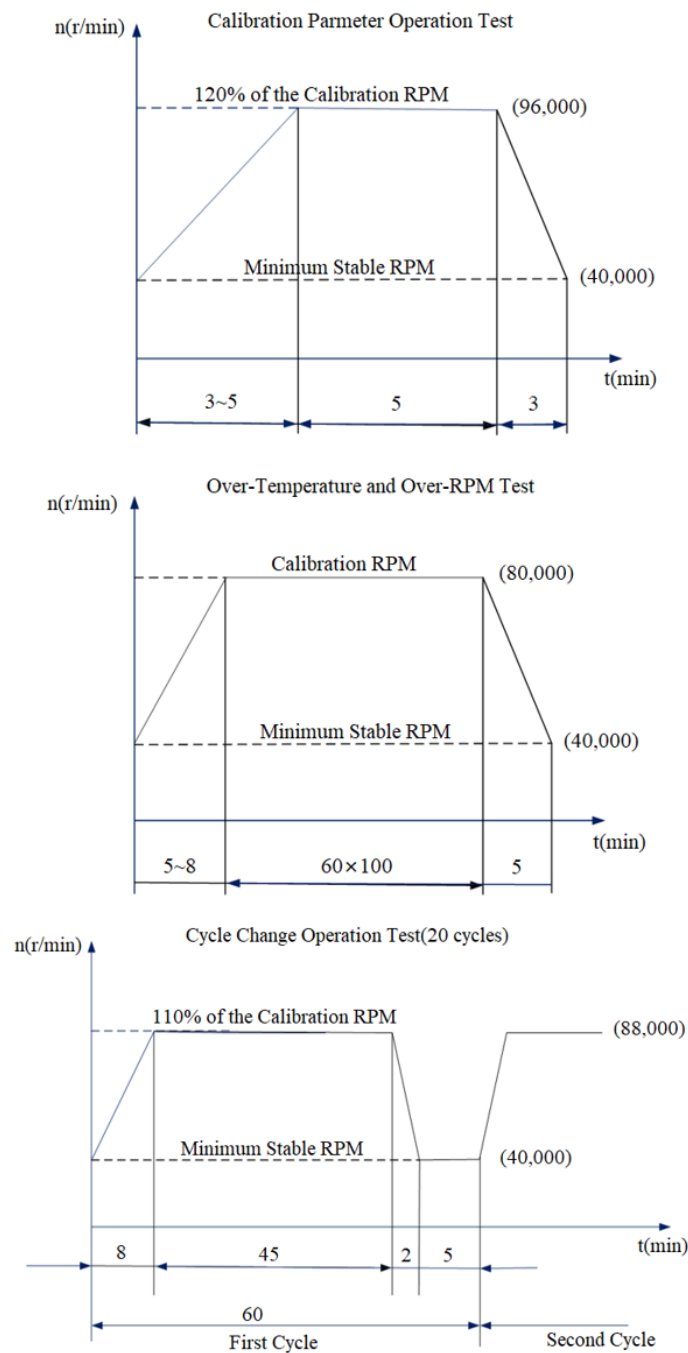


Figure 2. The 120-h turbocharger standard structure assessment test profile.

Combined with the analysis of the above test profiles, it is known that:

(1) Supercharger turbines often operate under high-speed and high-temperature loading conditions. These time-varying loads subject the turbine to various constraints all the time. One of the most important constraints in the optimization of a turbine’s aerodynamic performance is fatigue. Durable performance and fatigue life are the essential properties of engineered parts. The former is assessed by the endurance limit, generally throughout the assessment test cycle, while the latter is measured by the number of cycles of experience before it fails. High-period fatigue of a turbocharger is fatigue damage caused by the accumulation of alternating stresses caused by resonance. The resonance frequency range is from thousands of Hz to tens of thousands of Hz, but its design cycle life requirement is greater than 10^{10} . Therefore, the resonance problem has been solved by some effective methods. A specific analysis is as follows:

- As shown in Figure 2, the 120-h turbocharger standard structure assessment test includes three stages: (i) The first stage is the 100-h endurance performance test under constant stress. (ii) The second stage is the 5-min over-temperature and over-velocity test. (iii) The third stage is the 20-cycle alternating stress test. The endurance performance is assessed throughout the whole test cycle. However, the 20 cycles of the alternating stress test are very limited for fatigue performance assessment. Therefore, the assessment of endurance performance for a turbine impeller is more important in this case.
- As can be seen in Table 1, the test profile of the 350-h complete machine test for a diesel engine is mainly composed of four working conditions. Condition 1 is the calibration speed, and the torque is in accordance with the external characteristics. Condition 2 is 85–90% of the standard speed, and the torque is in accordance with the external characteristics. Condition 3 is 80% of the standard speed, and the torque is per the external characteristics. Condition 4 is the maximum torque speed, and the torque is the maximum torque. Condition 1–Condition 3 account for a high percentage of the entire test cycle, and the supercharger speed is generally not high during the no-load operation. In addition, the test is conducted in one cycle of 10 h, with 35 cycles in total. For a turbine impeller, the alternating stress test is very limited for fatigue performance assessment. Therefore, the test also mainly assesses the endurance performance of a turbine impeller.

(2) From the whole test profile, turbine impeller failure is mainly caused by the centrifugal load action associated with the speed of a supercharger. In addition, the material of a turbine impeller is the cast high-temperature alloy K418. The effect of high temperature causes the lasting limit (lasting strength) of the blade root to decrease continuously. From the point of view of material damage principles, this reduction in strength can be quantitatively described by the amount of damage and is monotonic with time. Therefore, the strength damage at the endurance limit or endurance stress can be used as the degradation parameter when analyzing the performance degradation trend of turbine impellers, as well as when evaluating the durability of superchargers. The endurance limit data of K418 at different temperatures and times are shown in Table 2. In this table, the relationship between the temperature, endurance limit, and life (duration) is indicated, and the relationship between the accumulated load, temperature, endurance limit, and life (duration) is implied. From Figure 1, we can see that the main stresses affecting the turbocharger turbine blade roots are the centrifugal and thermal loads. According to Table 2, temperature directly affects the material’s endurance limit, while rpm is directly linked to the endurance limit. The endurance limit is the main index for a durability assessment, and so temperature and rpm can be selected as the two sensitive stresses for the assessment test.

Table 2. Persistence limits of the K418 alloy at different temperatures and times [28].

Sampling	$\theta/^\circ\text{C}$	$\sigma_{t/h}/\text{MPa}$								
		σ_{50}	σ_{100}	σ_{200}	σ_{300}	σ_{500}	σ_{1000}	σ_{2000}	σ_{5000}	$\sigma_{10,000}$
Precision cast test rod	650	—	833	820	810	804 [Ⓛ]	774 [Ⓛ]	—	—	—
	700	810	725	720	710	666	627 [Ⓛ]	610 [Ⓛ]	—	—
	732	710	666	650	630	588	549	530 [Ⓛ]	470 [Ⓛ]	441 [Ⓛ]
	750	680	617	610	600	539	510	480	412 [Ⓛ]	372 [Ⓛ]
	800	560	480	470	460	412	363	340	294	255 [Ⓛ]
	816	540	441	430	400	363	323	300 [Ⓛ]	255 [Ⓛ]	235 [Ⓛ]
	850	410	372	350	310	294	265	240 [Ⓛ]	206 [Ⓛ]	167 [Ⓛ]
	900	300	274	250	230	216	176	160	137	108 [Ⓛ]
	930	250	216	190	180	167 [Ⓛ]	137 [Ⓛ]	—	—	—
	950	230	167	155	150	137	118 [Ⓛ]	100 [Ⓛ]	—	—
	982	170	137	125	120	108 [Ⓛ]	88 [Ⓛ]	—	—	—
	1000	140	118	113	110	88 [Ⓛ]	—	—	—	—

[Ⓛ] Data derived from the integrated curve of thermal intensity parameters.

3. The Performance Degradation Model Based on a BP Neural Network

3.1. Data Process

In accordance with the supercharger 120-h test (Table 3) and the complete engine 350-h test (Table 4), the results of the turbo–solid coupling simulation test are as shown in Tables 5 and 6.

Table 3. Data for the 120-h assessment test.

RPM	The Total Temperature at the Outlet	Total Pressure at the Outlet	Total Pressure at the Inlet
r/min	K	KPa	KPa
46,000	969	100	54
80,000	959	100	272
88,000	919	100	389
96,000	1050	100	495

Table 4. Data for the 350-h assessment test.

RPM	Total Temperature at the Outlet	Total Pressure at the Outlet	Total Pressure at the Inlet
r/min	K	KPa	KPa
72,000	923	100	250
64,000	923	100	220

Table 5. Fluid–solid coupling simulation results of the 120-h turbine test.

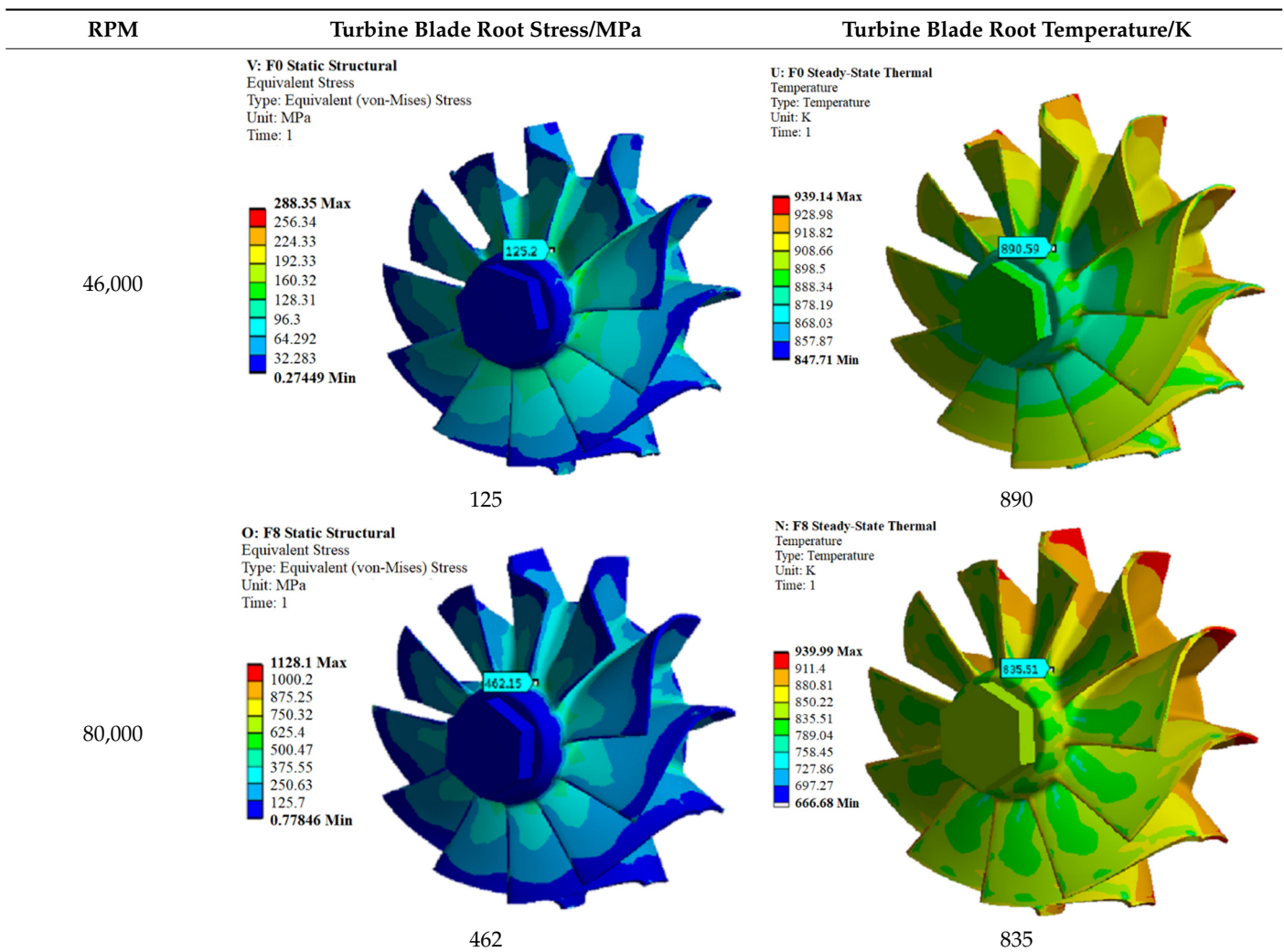


Table 5. Cont.

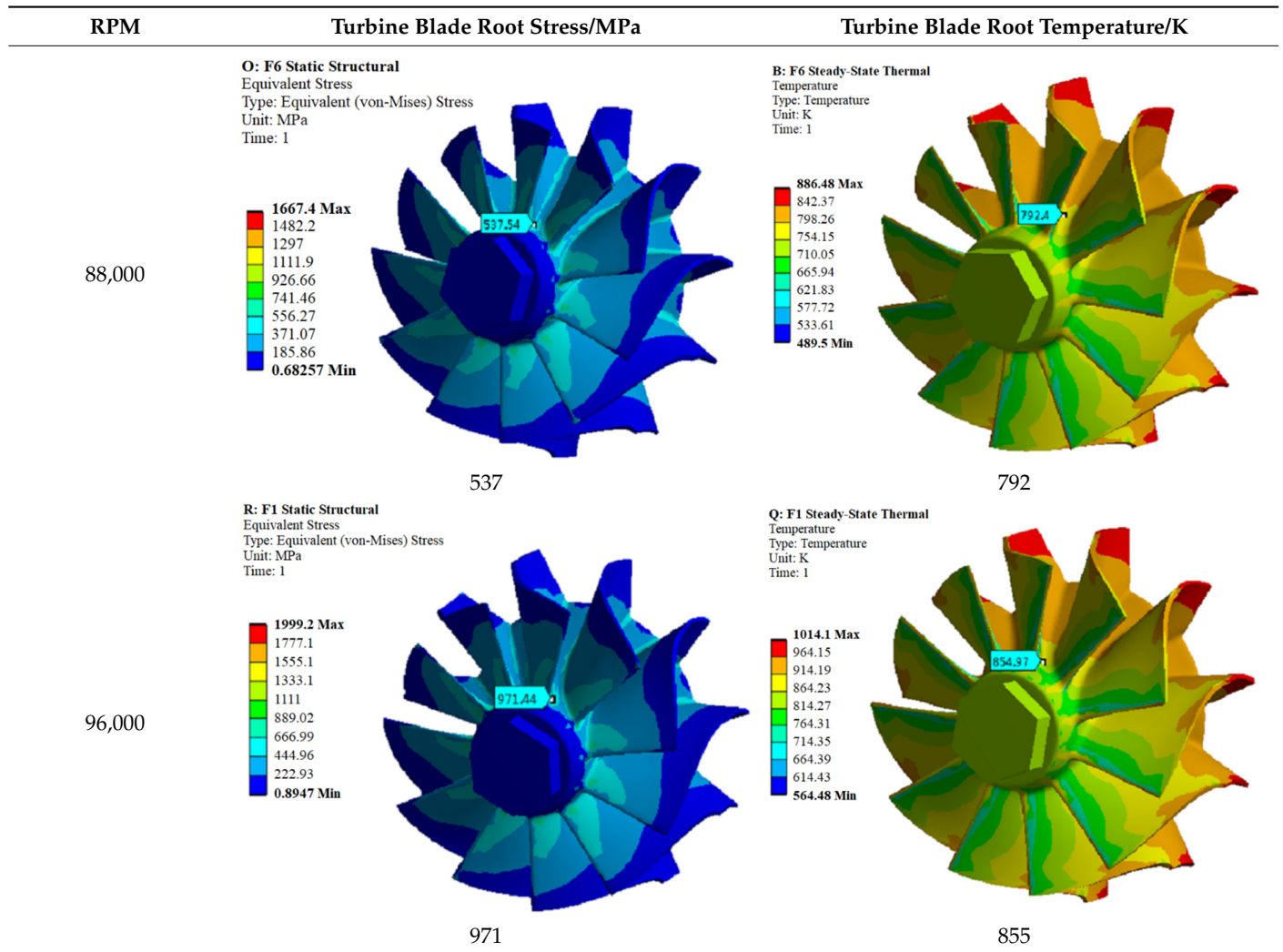


Table 6. Fluid–solid coupling simulation results of the 350-h turbine test.

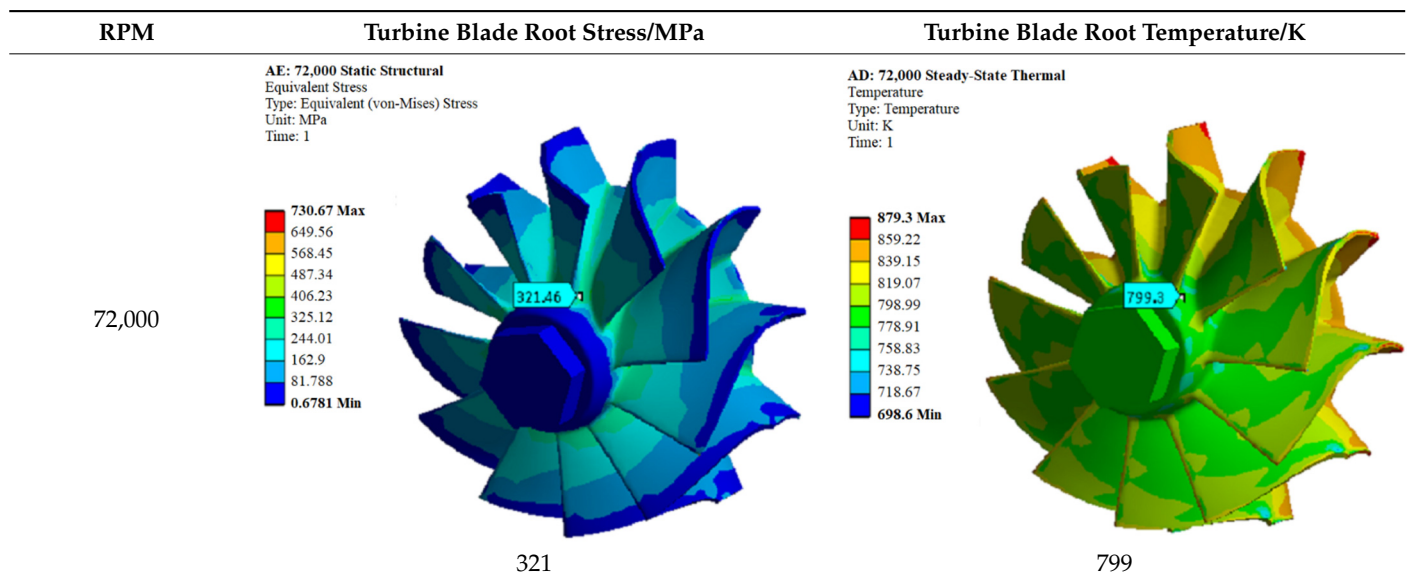
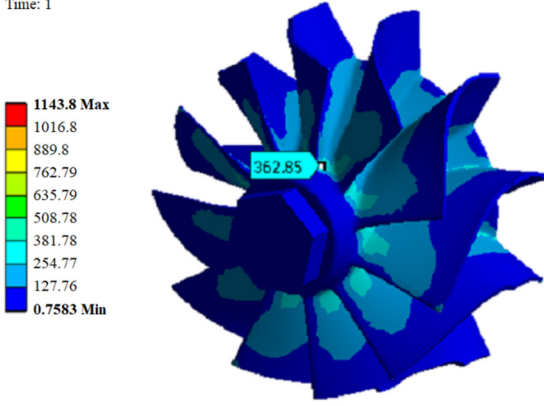
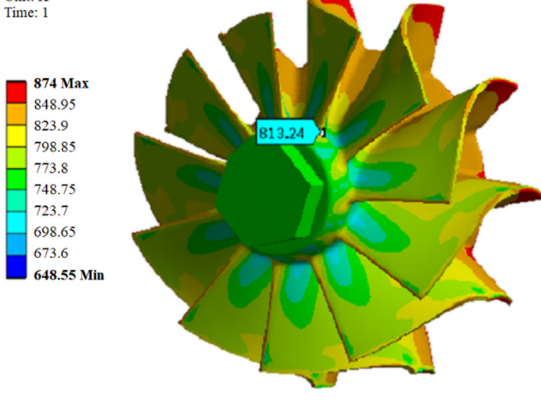


Table 6. Cont.

RPM	Turbine Blade Root Stress/MPa	Turbine Blade Root Temperature/K
64,000	<p>AE: 64,000 Static Structural Equivalent Stress Type: Equivalent (von-Mises) Stress Unit: MPa Time: 1</p>  <p>1143.8 Max 1016.8 889.8 762.79 635.79 508.78 381.78 254.77 127.76 0.7583 Min</p> <p>362.85</p> <p>363</p>	<p>AD: 64,000 Steady-State Thermal Temperature Type: Temperature Unit: K Time: 1</p>  <p>874 Max 848.95 823.9 798.85 773.8 748.75 723.7 698.65 673.6 648.55 Min</p> <p>813.24</p> <p>813</p>

3.1.1. Data Expansion

The accuracy of the nonlinear fitting of BP neural networks requires large numbers of valid data. However, the data sample size of this test is small. To solve the problem, we first need to establish the mathematical relationship between the amount of degradation and the sensitive stress according to the material property data (Table 2). Then, combining the above established mathematical function with the test date, the degradation model under each test condition can be derived.

The endurance performance is assessed throughout the life cycle of the whole test. The cumulative amount of stress σ at the action time t is recorded as the accumulated load $L(t)$. The relationship between the three can be expressed as follows:

$$\sigma_t = f(L(t), \theta) \tag{1}$$

where θ is the temperature and $L(t) = \sigma_i t$ or σ_i is the persistence limit.

The model accuracy of the neural network greatly depends on the sample data. To reduce the influence of the randomness of the original data, the information of regularity in the data is highlighted and improves the model's stability. The Larson–Miller formula is used to expand the existing data, and is given as follows:

$$P(\sigma) = T(C + \lg t) \times 10^{-3} \tag{2}$$

where σ (MPa) is the stress on the material, T (K) is the temperature, t (h) is the time, C is the material constant, and $P(\sigma)$ is the Larson–Miller parameter, in which the relationship between P and σ is given as follows:

$$\lg \sigma = a_2 P^2 + a_1 P + a_0 \tag{3}$$

where a_i ($i = 0, 1, 2$) is the coefficient.

For the selection of C , we use TAE (trial-and-error) to take values in the appropriate range. Using the data in Table 2 and combining Equations (2) and (3), the variation relationship between the GOF (goodness-of-fit) of R^2 and C is as shown in Figure 3.

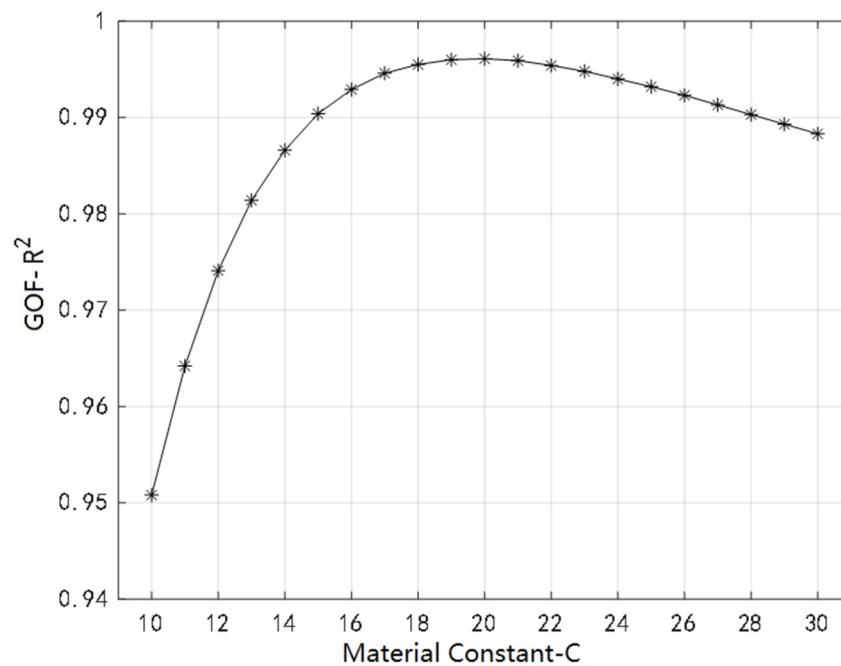


Figure 3. C – R² relation curve.

When C = 20.3, we can obtain MAX{R_i²} = 0.9962 and RMSE = 0.01708 (root mean square error). We can see the GOF of this model is very close to 1 and the RMSE is small, which can better reflect the relationship between the parameter P and the stress σ. Then, from Equations (2) and (3), we can derive:

$$\lg\sigma = -0.007822P^2 + 0.2744P + 0.6002 \tag{4}$$

$$P(\sigma) = T(20.3 + \lg t) \times 10^{-3} \tag{5}$$

Because test results rely on low-temperature data, the temperature is expanded toward the lower range. Taking T/°C = [500, 1000] and t/h = [50, 1000], and keeping the initial data and the step size as 10, we then combine Equation (4) with Equation (5), and the data can be expanded. The expanded sample has 3492, which is approximately 50 times the original data. We choose these data as the neural network training data.

3.1.2. Data Normalization

The three types of data included in the training data have different magnitudes and large differences in values. These are not suitable for direct use in nonlinear fitting. To keep these different magnitudes in the same order of magnitude and improve the convergence of the algorithm, the available data are normalized to the interval [-1, 1] using the following equation:

$$x_{mid} = \frac{x_{max} + x_{min}}{2}, \bar{x}_i = \frac{x_i - x_{mid}}{\frac{1}{2}(x_{max} - x_{min})} \tag{6}$$

3.2. Construction of a Turbine Performance Degradation Model Based on the Material Endurance Limit

Before constructing the model, we need to determine the basic parameters and algorithms for training the model. This mainly includes determining the neural network structure and selecting the learning parameters, excitation function, and transfer function, and then setting the basic elements in the genetic algorithm.

3.2.1. Define the Network Structure

The model takes the temperature and accumulated load as inputs in which the node $n = 2$, and it takes the lasting strength as an output in which the node $m = 1$. The input layer, hidden layer, and output layer of the network are all single-layer structures. Too few nodes in the hidden layer will reduce the accuracy of the model, and too many nodes will cause overfitting. An empirical formula is adopted in this paper, as follows:

$$k = 2n + 1 \quad (7)$$

where n is the number of input layer nodes. The number of hidden layer nodes determined by Equation (7) is 5; therefore, the neural network structure used in this paper is 2-5-1.

3.2.2. Determine the Network Parameter

The proportion of training set, verification set, and test set in the sample data are 75%, 15%, and 15%, respectively. The initial weights and thresholds of the network are first chosen randomly at $[-1, 1]$. The optimal weights will be determined later by the genetic algorithm. The maximum number of iterations is 2000, the expected error is 0.00001, and the learning rate is 0.1. The performance metric of the network is the MSE (mean squared error).

3.2.3. Select the Excitation Function

The three commonly used excitation functions in MATLAB's Neural Net Fitting toolbox are the *logsig*, *tansig*, and *purelin* functions. The *logsig* function is a unipolar S-type nonlinear transfer function with an unlimited input range and an output range of $(0, 1)$. The *tansig* function is a bipolar S-type nonlinear transfer function with an unlimited input range and an output range of $(-1, 1)$. The *purelin* function is a linear transfer function with an unlimited range of inputs and outputs. In this paper, all data have been normalized to $[-1, 1]$. To ensure the output range, *tansig* and *purelin* are selected as the transfer functions for the neurons in the implicit and output layers, respectively.

3.2.4. Select the Training Algorithm

The commonly used training algorithms in MATLAB are *trainlm*, *trainbr*, and *trainscg*. Using the trial-and-error method, we combine different statistical criteria to select the training algorithm which is more suitable for the model. These criteria include iterations, the mean square error (MSE), the goodness of fit (GOF-R2), and the root mean square error (RMSE). The calculation formulas are as follows:

$$\text{MSE} = \frac{1}{n} \sum_{i=1}^n (f_{ANN,i} - f_i)^2 \quad (8)$$

$$R^2 = 1 - \frac{\sum_{i=0}^n (\hat{f}_{ANN,i} - f_i)^2}{\sum_{i=0}^n (\bar{f} - f_i)^2} \quad (9)$$

$$\text{RMSE} = \sqrt{\frac{1}{n} \sum_{i=1}^n (f_{ANN,i} - f_i)^2} \quad (10)$$

The results are shown in Table 7.

Table 7. Training results of the three algorithms.

Training Algorithm	Iterations	MSE	GOF-R ²	RMSE
trainlm	19	0.996×10^{-5}	0.99994	3.155×10^{-3}
trainbr	106	0.977×10^{-5}	0.99994	3.126×10^{-3}
trainscg	189	0.983×10^{-4}	0.99937	9.915×10^{-3}

From the Table, it can be seen that the GOF and MSE of the three algorithms have no significant differences, while trainlm has the least iterations and the fastest convergence speed. To improve the learning efficiency of the network, this paper chooses trainlm as the training algorithm.

3.2.5. Determine the Basic Elements of the GA

The structure of the BP neural network in this paper is 2-5-1. The weight and threshold are shown in Table 8.

Table 8. Numbers of the weight and threshold.

Connection Weights of the Input Layer and the Implied Layer	Threshold of the Implied Layer	Connection Weights of the Implicit Layer and the Output Layer	Threshold for the Output Layer
10	5	5	1

In this paper, individuals are coded in real numbers. Each encoding consists of weights and thresholds, and the length is 21. The iteration of the algorithm is 30, the population size is 20, the crossover probability is 0.7, and the variance probability is 0.1.

The fitness function is determined by the absolute value of the sum of the errors between the predicted and expected outputs of the neural network prediction model outputs. The calculation formula is as follows:

$$F = \sum_{i=1}^n abs(y_i - d_i) \quad (11)$$

where F is the fitness value, y_i is the predicted output of the neural network, and d_i is the expected output.

According to the above formula, the lower the fitness is, the smaller the prediction error is, and the higher the probability of its selection should be. The calculation formula is:

$$P_i = \frac{\frac{1}{F_i}}{\sum_{j=1}^n \frac{1}{F_j}} \quad (12)$$

3.2.6. Modeling

Modeling is established based on the above model information. It can obtain the nonlinear model $f(net)$ that can effectively reflect the accumulated load, temperature, and action time, which can be expressed as:

$$\sigma = f(L(t), \theta) \quad (13)$$

3.3. Turbine Endurance Limit Calculation Model

The two types of test data obtained from Tables 5 and 6 are shown in Tables 9 and 10, respectively.

Table 9. The 120-h test data.

Number	$n/r \cdot \text{min}^{-1}$	Time t/h	Temperature T/K	Turbine Hazardous Area Stress σ/MPa
1	80,000	100	835	462
2	96,000	0.0833	855	971
3	88,000	20	792	537

Table 10. The 350-h test data.

Number	$n/r \cdot \text{min}^{-1}$	Time t/h	Temperature T/K	Turbine Hazardous Area Stress σ/MPa
1	95,500	60	756	538
2	87,000	420	771	434
3	81,800	100	798	371
4	76,200	20	824	303

If we denote the stress in each stage as $\sigma_i (i = 1, 2, \dots)$, then the corresponding cumulative load $L_i(t)$ can be expressed as:

$$L_i(t) = \sum_{i=1}^{n-1} \sigma_i t_i + \sigma_n (t_n - t_{n-1}) \tag{14}$$

Combining the test temperature θ_i at each stage and substituting it into Equation (13), we can obtain the calculation model of the endurance limit for each test process, respectively, as:

$$\sigma_{120} = f(L_{120}(t), \theta_{120}) \tag{15}$$

$$\sigma_{350} = f(L_{350}(t), \theta_{350}) \tag{16}$$

The relationship between the endurance limit and time during the test is respectively fitted, as shown in Figures 4 and 5.

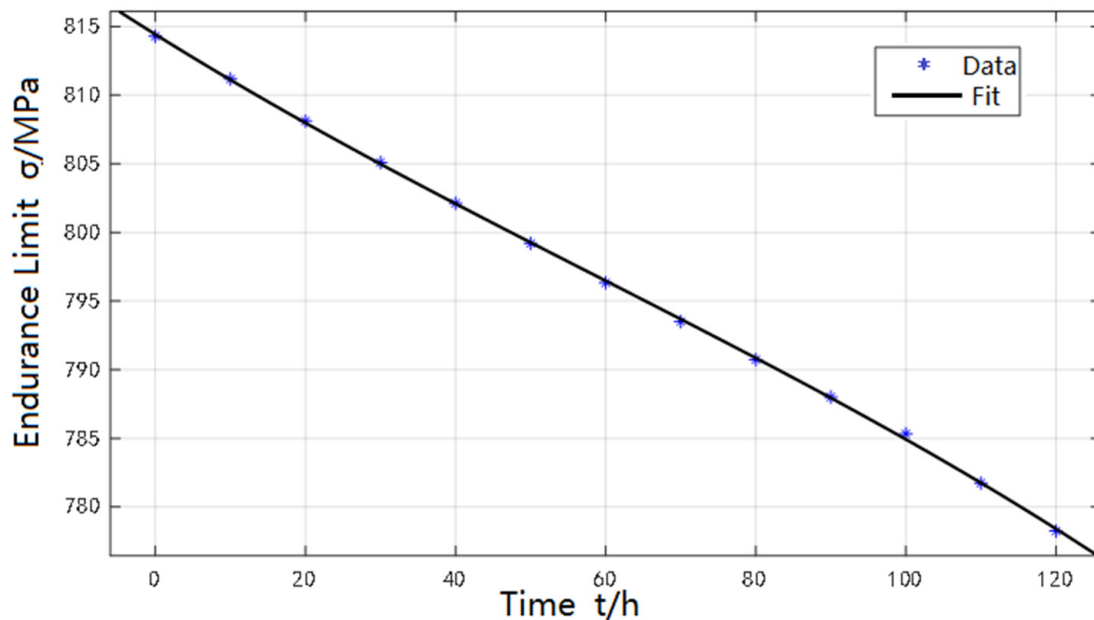


Figure 4. The 120 h test endurance limit–time curve.

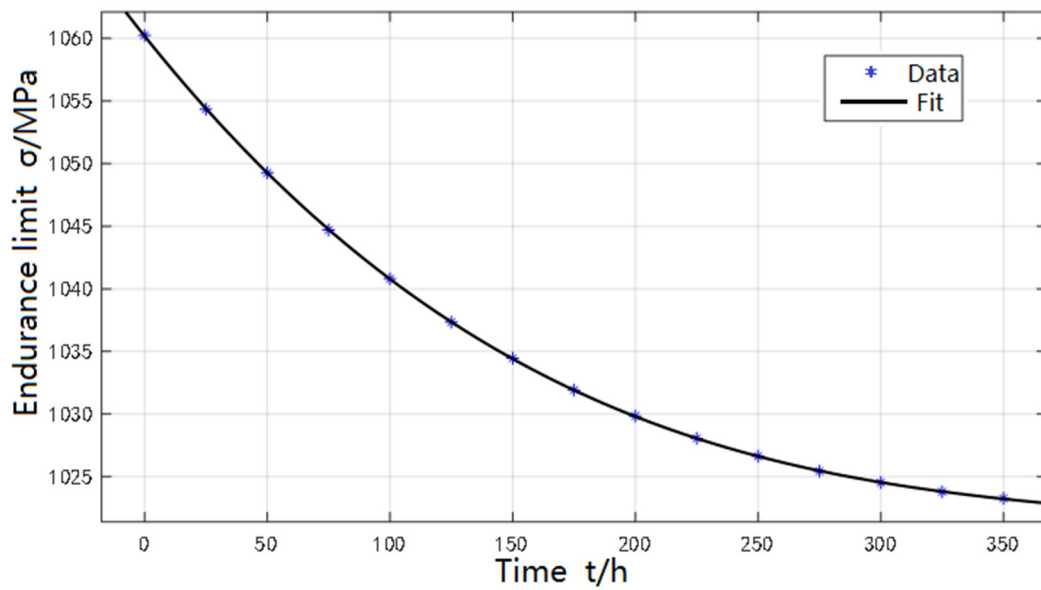


Figure 5. The 350 h test endurance limit–time curve.

From the above figures, it can be concluded that the endurance limit tends to decay slowly with time during the test, and after the test, the endurance limits are $\sigma_{120} \approx 778$ MPa and $\sigma_{350} \approx 1023$ MPa.

4. Results Analysis

4.1. Model Validity

The variation of the fitness of the optimal individual during the calculation of the genetic algorithm is shown in Figure 6. The optimal solution or local optimal solution is derived after approximately 17 iterations.

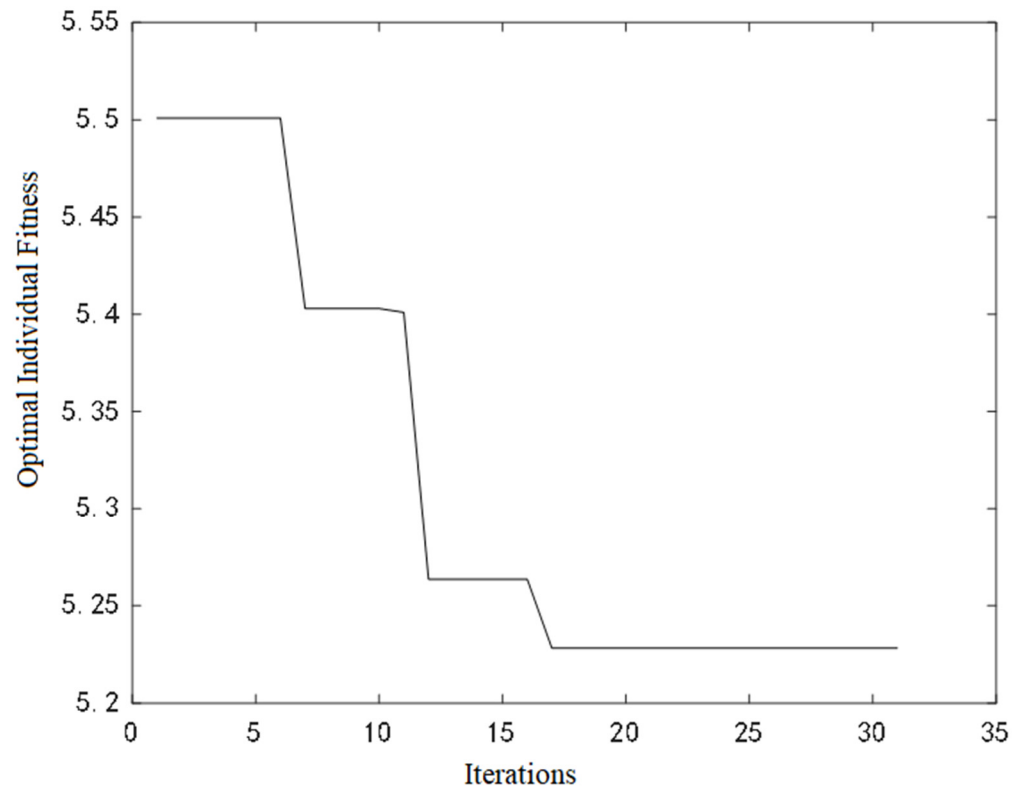


Figure 6. Optimal individual fitness curve.

Taking the optimized data as the initial weights and thresholds of the BP neural network, after 76 iterations, the EE (expected error) is determined and we can obtain $MSE = 0.999 \times 10^{-5}$ and $R^2 = 0.99994$. The results are shown in Figures 7 and 8.

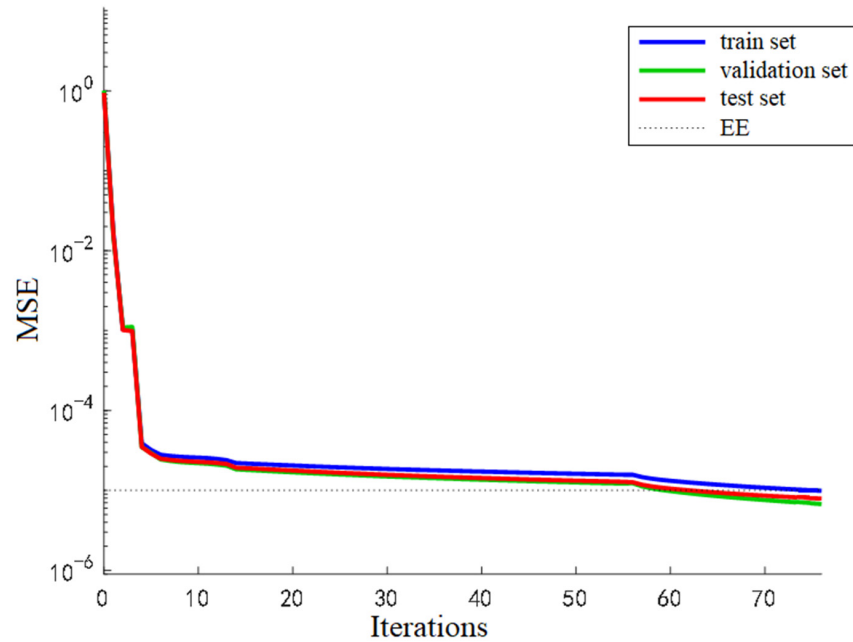


Figure 7. Training error curve.

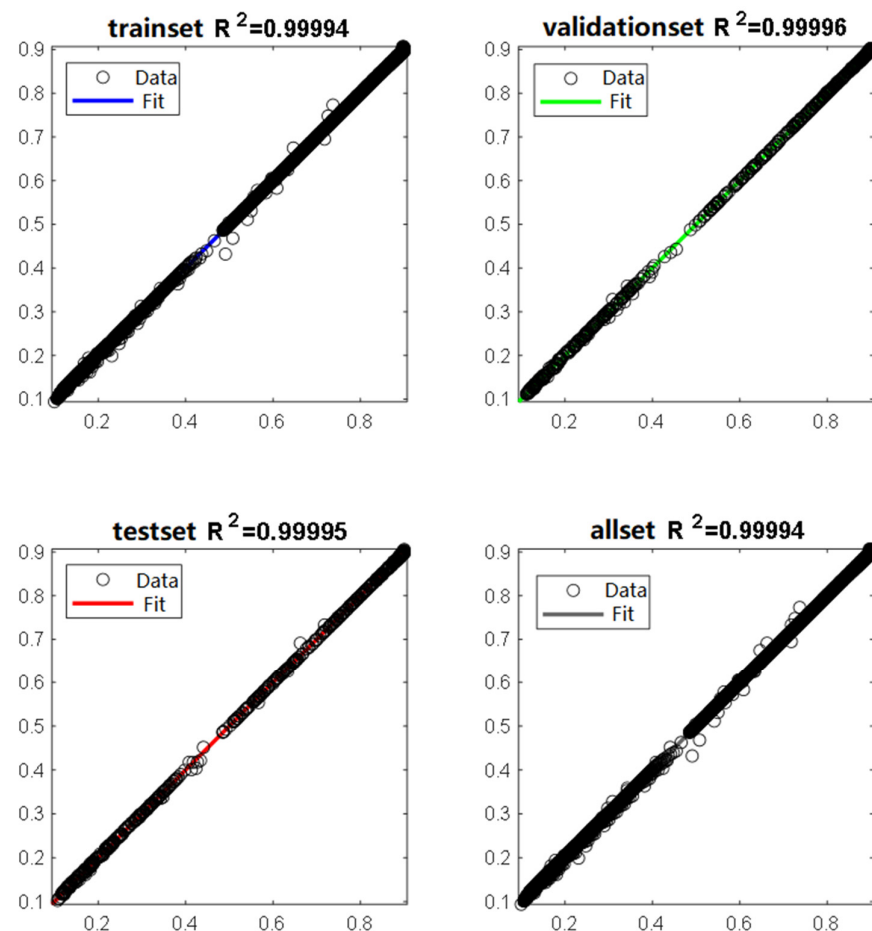


Figure 8. Model's GOF.

The final error of the model is small and the GOF is close to 1. We can conclude that the model can effectively reflect the nonlinear relationship between the accumulated load, temperature, and action time.

4.2. Model Application

Based on the above-mentioned performance degradation model of the turbine impeller studied for the bench test, this paper discusses the above Problem I and Problem II.

4.2.1. Discussion of Problem I

Problem I is a mathematical explanation of why the 120-h structural test of the supercharger meets the 350-h test of the engine. Based on the degradation model of the endurance limit of the 120-h and 350-h tests, we obtained $\sigma_{120} = 778$ MPa and $\sigma_{350} = 1023$ MPa at the end of the tests. The analysis suggests that the true stress undergone during the 120-h calibration parameter test is assumed to be P_{120} . If the 120-h assessment test is passed, it means that the true stress P_{120} should be less than σ_{120} , i.e., $P_{120} < \sigma_{120} = 778$ MPa. According to the design and simulation results of the 350-h test, the RPM and temperature of this test are less than those of the 120-h structural test. In theory, the real stresses in the 350-h test should be less than those of the 120-h test, i.e., $P_{350} < P_{120}$. It is concluded that when the 120-h structural assessment test is passed, the endurance limit of both has the following relationship: $P_{350} < P_{120} < \sigma_{120} = 778$ MPa. After the 350-h test, $\sigma_{350} = 1023$ MPa and the following relationship exists: $P_{350} < P_{120} < \sigma_{120} < \sigma_{350}$. This indicates that the real stress on the supercharger during the 350-h complete test must be less than that of the endurance limit under the current test conditions, and the test must pass.

4.2.2. Discussion of Problem II

Problem II is the design suggestions for the structural assessment test of the supercharger for a turbine impeller. As can be seen from the test protocols for the 120-h structural test and the 350-h complete test of the supercharger, the sensitive parameters (temperature and speed) are different for both tests, and thus the cumulative load is different. Firstly, we should calculate the cumulative load ratios for the 350-h test and 120-h test. Secondly, we should calculate the cumulative load for the new complete engine test and use the load ratios to obtain the cumulative load required for the new test of the supercharger. Then, we will need to improve the test profile based on the 120-h calibration parameters. Finally, based on the above degradation model, we can verify that the new assessment test of the supercharger meets the new complete engine test requirements. We can take the change of the complete engine assessment test to 500 h as an example:

- Calculate the cumulative load ratio. According to the 120-h structural test and 350-h complete machine test, it can be calculated that the cumulative load ratio is: $L_{120}/L_{350} = 0.4467$.
- Calculate the cumulative load required for the new structural assessment test. According to the ratio 0.4467, when the complete engine test reaches 500 h, the 350 h test is designed to do 50 cycles. Then, one can calculate the cumulative load of the required supercharger structure assessment experiment.
- Design the new supercharger assessment test. The 120 h calibration parameter assessment test is roughly divided into two stages. The first stage (5/6) is the uniform speed rotation. The second stage (1/6) applies the alternating stress. Based on the rotation speed, it is calculated that the test time of the supercharger structure assessment required to pass the 500 h complete engine test is 172 h.
- Validation based on the degradation model. According to the method in Section 3 of this paper, $\sigma_{172} = 767$ MPa $< \sigma_{500} = 1014$ MPa; that is, the supercharger's 172 h of structural assessment can meet the requirements of the 500 h complete machine test assessment.

- Suggestions for the design of the 500-h assessment test: to facilitate the actual operation of the project, it is recommended to use a multiple of 10 as the actual intensive assessment time, i.e., take the assessment time of 180 h.

5. Conclusions

In this paper, combining the characteristics of accelerated life test data analysis and intensive testing to quickly achieve performance degradation or to expose failures, we proposed an accelerated degradation durability evaluation model for the turbine impeller of a turbine based on a GA-BP Neural Network. The specific work is summarized as follows:

- Firstly, in terms of model-building ideas, we combined the failure mechanism and bench test analysis, and the endurance limit was determined as the degradation quantity, which could effectively avoid the difficulty of observing and measuring the degradation quantity of the traditional method, which selects the wear quantity and wear size for the degradation analysis of mechanical products. Meanwhile, the temperature and RPM were selected as the sensitive monitoring parameters.
- Then, in terms of modeling methods, based on the turbine material endurance limit data, we obtained a large amount of sample data by resampling as the input quantity and target quantity for training, which helped to ensure the model's accuracy. Based on the GA-BP neural network, the nonlinear relationship between the endurance limit and the cumulative load temperature was fitted, which effectively avoided the problem that the traditional method needs to solve a complex system of likelihood equations, and it could map the mathematical relationship between variables well. Then, the performance degradation model of the turbine impeller during the test was provided to realize the evaluation of the endurance limit.
- Finally, in terms of model applications, we analyzed the validity of the model, and based on the model calculation results, we reasonably explained whether the current structural assessment test for turbochargers (according to the component level) could meet the requirements of the complete engine assessment test. Meanwhile, we illustrated how the corresponding component-level assessment test time should be adjusted when the whole engine test time is adjusted. In other words, using the proposed model for the scientific explanation of the above two types of problems can provide technical support for the design of the critical component-level assessment test in a turbocharger durability assessment, thus effectively controlling the cost of a turbocharger durability assessment test and providing guidance for other similar problems.

Author Contributions: Conceptualization, X.Y. and Z.W.; methodology, X.Y. and Z.W.; software, X.Y.; validation, X.Y., Z.W., S.L., X.H. and Q.T.; formal analysis, X.Y., Z.W. and S.L.; investigation, X.Y., Z.W. and S.L.; resources, X.Y., Z.W., S.L., X.H. and Q.T.; data curation, X.Y. and Z.W.; writing—original draft preparation, X.Y. and Z.W.; writing—review and editing, X.Y., Z.W. and S.L.; visualization, X.Y. and Z.W.; supervision, X.Y.; project administration, X.Y.; funding acquisition, X.Y. All authors have read and agreed to the published version of the manuscript.

Funding: This research received no external funding.

Institutional Review Board Statement: Not applicable.

Informed Consent Statement: Not applicable.

Data Availability Statement: The data that support the findings of this study are available from the corresponding author upon reasonable request.

Acknowledgments: This paper is supported by the Special Fund of the Ministry of Industry and Information Technology of the People's Republic of China. The authors are grateful to the chief editor, editor, and reviewers for the suggestions, which improved the paper.

Conflicts of Interest: The authors declare no conflict of interest.

References

1. Zengquan, W.; Zheng, W. *Structural Reliability of Automotive Turbocharger*; Beijing Science Press: Beijing, China, 2013; p. 305. (In Chinese)
2. Daxin, Z. *Turbocharging and Turbochargers*; China Machine Press: Beijing, China, 1992; p. 548. (In Chinese)
3. Meeker, W.Q.; Hamada, M. Statistical tools for the rapid development and evaluation of high-reliability products. *IEEE T. Reliab.* **1995**, *44*, 187–198. [[CrossRef](#)]
4. Jiao, J.; De, X.; Chen, Z.; Zhao, T. Integrated circuit failure analysis and reliability prediction based on physics of failure. *Eng. Fail. Anal.* **2019**, *104*, 714–726. [[CrossRef](#)]
5. Xu, J.; Wang, L.; Li, Y.; Zhang, Z.; Wang, G.; Hong, C. A unified MMC reliability evaluation based on physics-of-failure and SM lifetime correlation. *Int. J. Electr. Power Energy Syst.* **2019**, *106*, 158–168. [[CrossRef](#)]
6. Xu, D.; Wei, Q.; Chen, Y.; Kang, R. Reliability Prediction Using Physics-Statistics-Based Degradation Model. *IEEE Trans. Compon. Packag. Manuf. Technol.* **2015**, *5*, 1573–1581.
7. Lu, L.; Wang, B.; Hong, Y.; Ye, Z. General Path Models for Degradation Data with Multiple Characteristics and Covariates. *Technometrics* **2021**, *63*, 354–369. [[CrossRef](#)]
8. Veloso, G.A.; Loschi, R.H. Dynamic linear degradation model: Dealing with heterogeneity in degradation paths. *Reliab. Eng. Syst. Saf.* **2021**, *210*, 107446. [[CrossRef](#)]
9. Firoozeh, H.; Mikhail, N. On the linear degradation model with multiple failure modes. *J. Appl. Stat.* **2010**, *37*, 1499–1507.
10. Chen, X.; Sun, X.; Ding, X.; Tang, J. The inverse Gaussian process with a skew-normal distribution as a degradation model. *Commun. Stat. Simul. Comput.* **2020**, *49*, 2827–2843. [[CrossRef](#)]
11. Aryal, G.R.; Pokhrel, K.P.; Khanal, N.; Tsokos, C.P. Reliability Models Using the Composite Generalizers of Weibull Distribution. *Ann. Data Sci.* **2019**, *6*, 807–829. [[CrossRef](#)]
12. Fuqing, Y.; Barabadi, A.; Jinmei, L. Reliability modelling on two-dimensional life data using bivariate Weibull distribution: With case study of truck in mines. *Eksplorat. Niezawodn. Maint. Reliab.* **2017**, *19*, 650–659. [[CrossRef](#)]
13. Kudryavtsev, A.A.; Titova, A.I. Bayesian queuing and reliability models: Degenerate-Weibull case. *Inform. Its Appl.* **2016**, *10*, 68–71.
14. Li, N.; Lei, Y.; Yan, T.; Li, N.; Han, T. A Wiener-Process-Model-Based Method for Remaining Useful Life Prediction Considering Unit-to-Unit Variability. *IEEE T. Ind. Electron.* **2019**, *66*, 2092–2101. [[CrossRef](#)]
15. Zhang, Z.; Si, X.; Hu, C.; Lei, Y. Degradation data analysis and remaining useful life estimation: A review on Wiener-process-based methods. *Eur. J. Oper. Res.* **2018**, *271*, 775–796. [[CrossRef](#)]
16. Zhai, Q.; Ye, Z. RUL Prediction of Deteriorating Products Using an Adaptive Wiener Process Model. *IEEE T. Ind. Inform.* **2017**, *13*, 2911–2921. [[CrossRef](#)]
17. Wang, Y.F.; Huang, Y.; Liao, W.C. Degradation analysis on trend gamma process. *Qual. Reliab. Eng. Int.* **2021**, *38*, 941–956. [[CrossRef](#)]
18. Duan, F.; Wang, G. Optimal design for constant-stress accelerated degradation test based on gamma process. *Commun. Stat. Theory Methods* **2019**, *48*, 2229–2253. [[CrossRef](#)]
19. Rodríguez-Picón, L.A.; Rodríguez-Picón, A.P.; Méndez-González, L.C.; Rodríguez-Borbón, M.I.; Alvarado-Iniesta, A. Degradation modeling based on gamma process models with random effects. *Commun. Stat. Simul. Comput.* **2018**, *47*, 1796–1810. [[CrossRef](#)]
20. Park, S.; Kim, J. Application of gamma process model to estimate the lifetime of photovoltaic modules. *Sol. Energy* **2017**, *147*, 390–398. [[CrossRef](#)]
21. Li, L.; Wan, H.; Gao, W.; Tong, F.; Li, H. Reliability based multidisciplinary design optimization of cooling turbine blade considering uncertainty data statistics. *Struct. Multidiscip. Optim.* **2019**, *59*, 659–673. [[CrossRef](#)]
22. Zhu, S.; Liu, Q.; Lei, Q.; Wang, Q. Probabilistic fatigue life prediction and reliability assessment of a high pressure turbine disc considering load variations. *Int. J. Damage Mech.* **2018**, *27*, 1569–1588. [[CrossRef](#)]
23. Zhou, J.; Huang, H.; Li, Y.; Guo, J. A framework for fatigue reliability analysis of high-pressure turbine blades. *Ann. Oper. Res.* **2022**, *311*, 489–505. [[CrossRef](#)]
24. Yue, P.; Ma, J.; Zhou, C.; Zu, J.W.; Shi, B. Dynamic fatigue reliability analysis of turbine blades under combined high and low cycle loadings. *Int. J. Damage Mech.* **2021**, *30*, 825–844. [[CrossRef](#)]
25. Zhang, C.; Wei, J.; Wang, Z.; Yuan, Z.; Fei, C.; Lu, C. Creep-Based Reliability Evaluation of Turbine Blade-Tip Clearance with Novel Neural Network Regression. *Materials* **2019**, *12*, 3552. [[CrossRef](#)] [[PubMed](#)]
26. Zhao, Q.; Yuan, Y.; Sun, W.; Fan, X.; Fan, P.; Ma, Z. Reliability analysis of wind turbine blades based on non-Gaussian wind load impact competition failure model. *Measurement* **2020**, *164*, 107950. [[CrossRef](#)]
27. Wang, Z.; Ma, T. Fatigue and Creep Life Prediction Method of Turbine Blades for Turbocharger. *China Mech. Eng.* **2019**, *30*, 2521–2526.
28. Manual, C.O.T.C. *Chinese Aeronautical Materials Manual*; Standards Press of China: Beijing, China, 2002.